Food & Function

ROYAL SOCIETY OF CHEMISTRY

PAPER

View Article Online
View Journal | View Issue





Cite this: *Food Funct.*, 2020, **11**, 7626

# Design of polymer-free Vitamin-A acetate/cyclodextrin nanofibrous webs: antioxidant and fast-dissolving properties†

Asli Celebioglu* and Tamer Uyar *

The encapsulation of food/dietary supplements into electrospun cyclodextrin (CD) inclusion complex nanofibers paves the way for developing novel carrying and delivery substances along with orally fast-dissolving properties. In this study, CD inclusion complex nanofibers of Vitamin-A acetate were fabricated from polymer-free aqueous systems by using the electrospinning technique. The hydroxypropylated (HP) CD derivatives of HPβCD and HPγCD were used for both encapsulation of Vitamin-A acetate and the electrospinning of free-standing nanofibrous webs. The ultimate Vitamin-A acetate/CD nanofibrous webs (NWs) were obtained with a loading capacity of 5% (w/w). The amorphous distribution of Vitamin-A acetate in the nanofibrous webs by inclusion complexation and the unique properties of nanofibers (*e.g.* high surface area and porosity) ensured the fast disintegration and fast dissolution/release of Vitamin-A acetate/CD-NW in a saliva simulation and aqueous medium. The enhanced solubility of Vitamin-A acetate in the case of Vitamin-A acetate/CD-NW also ensured an improved antioxidant property for the Vitamin-A acetate compound. Moreover, Vitamin-A acetate thermally degraded at higher temperature in Vitamin-A acetate/CD-NWs, suggesting the enhanced thermal stability of this active compound. Here, HPβCD formed inclusion complexes in a more favorable way when compared to HPγCD. Therefore, there were some uncomplexed Vitamin-A acetate crystals detected in Vitamin-A acetate/HPγCD-NW, while Vitamin-A acetate molecules loaded in Vitamin-A acetate/HPβCD-NW were completely in complexed and amorphous states. Depending on this, better solubilizing effect, higher release amount and enhanced antioxidant properties have been provided for the Vitamin-A acetate compound in the case of Vitamin-A acetate/HPβCD-NW.

Received 7th July 2020,
Accepted 19th August 2020

DOI: 10.1039/d0fo01776k

rsc.li/food-function

## 1. Introduction

The encapsulation of bioactive compounds such as vitamins, essential oils and flavors in functional food/dietary supplements is becoming an emerging research area.[1] The bioactive compounds are mostly hydrophobic with limited water solubility and they are often volatile and sensitive to environmental conditions.[1,2] Therefore, encapsulation of such bioactive compounds within hydrophilic biopolymer matrices enhances their water solubility and bioavailability and also increases their shelf-life by improving their stability against temperature, light and oxygen.[1] There are several methods for encapsulation of bioactive compounds such as emulsion, extrusion, co-precipitation, coacervation, spray-drying, freeze-drying, electrospraying and electrospinning.[1,3,4] Each encapsulation approach results in different structures and morphologies and therefore the physicochemical properties and delivery of these bioactive compounds would be different from each other. Among these encapsulation approaches, recently, electrospinning has been shown to be a very feasible one for encapsulation of bioactive compounds for various applications including food, pharmaceutical and cosmetic.[4–9] The solution electrospinning technique can enable the easy encapsulation of bioactive compounds by using their solution or dispersion with biopolymers at ambient conditions.[4–9] On the other hand, melt electrospinning, which requires high temperature to melt polymers, is a limited method, because there are few biopolymers that can be processed at high temperature. Moreover, high temperature can be problematic during melt electrospinning upon degrading and evaporating bioactive compounds.[10] Electrospinning generally produces fibers with a diameter of less than a micron and they are generally classified as nanofibers. The electrospun nanofibers are fabricated

*Department of Fiber Science & Apparel Design, College of Human Ecology, Cornell University, Ithaca, NY, 14853, USA. E-mail: ac2873@cornell.edu, tu46@cornell.edu*

†Electronic supplementary information (ESI) available. See DOI: 10.1039/d0fo01776k

in a nonwoven form having large surface area and highly porous structure.[11] Such lightweight, flexible, and free-standing nanofibrous webs which are electrospun from hydrophilic biopolymers can easily dissolve with water contact. Therefore, electrospun nanofibrous webs encapsulating bioactive compounds can be very feasible for developing fast-dissolving delivery systems for both the food and pharmaceutical industries. Very recently, we have shown that fast-dissolving nanofibrous webs of cyclodextrin (CD) inclusion complexes can be effectively produced from various compounds such as essential oils,[12–17] flavors,[18,19] dietary supplements,[20–23] and drugs[24–27] in the absence of a polymeric matrix. CDs are cyclic oligosaccharides obtained from starch, with the U.S. Food and Drug Administration classifying CDs as GRAS (Generally Recognized as Safe). CDs are quite applicable in both food and pharmaceutical industries due to their inclusion complexation ability and non-toxic nature.[28,29] The molecular encapsulation of active ingredients through CD inclusion complexation could enhance their solubility and bioavailability, mask the bitter taste, control their release, extend their shelf-life and prevent their loss.[28–31]

Vitamins have diverse biochemical functions and therefore they are used extensively in many areas including foods/feeds, pharmaceuticals, cosmetics, and biomedical applications.[32,33] As one of the retinoids, Vitamin-A can be found in foods as retinyl ester (retinyl palmitate and retinyl acetate) or retinol form and they are commonly employed as food/dietary supplements and nutraceutical products due to their wide range of biochemical activities.[34,35] As has been reported previously, the most prominent property of Vitamin-A is its antioxidant capacity, and therefore it may show potential for treatments of cancer,[36] diabetes,[37] dermatological disorders[38] and cardiovascular diseases.[39] Vitamin-A acetate (retinyl acetate) is one of the widely known and used derivatives of Vitamin-A having antioxidant property; however, it is a lipophilic compound with very limited water solubility and is very sensitive to oxidation and high temperature. Therefore, encapsulation of Vitamin-A acetate is of interest for effective delivery of such bioactive compound to improve its bioavailability and stability and enhance its nutritional value. As has been mentioned, CDs are well known as molecular encapsulation agents due to their inclusion complexation property where the water solubility, bioavailability and stability of various bioactive molecules are significantly improved.[40] The inclusion complexation of Vitamin-A derivatives with different types of CD has been reported.[41–43] The encapsulation of Vitamin-A acid,[44] Vitamin-A palmitate,[45,46] and Vitamin-A acetate[47] within polymeric electrospun nanofibers was also reported in order to control its delivery and/or increase its thermal stability. In the present study, we have aimed to develop fast-dissolving and antioxidant nanofibrous webs of Vitamin-A acetate/CD inclusion complexes by using two derivatives of CD (hydroxypropyl-beta-cyclodextrin (HPβCD) and hydroxypropyl-gamma-cyclodextrin (HPγCD)) (Fig. 1). The structure, dissolution/disintegration, release, and antioxidant potential of samples were examined by various analyses.

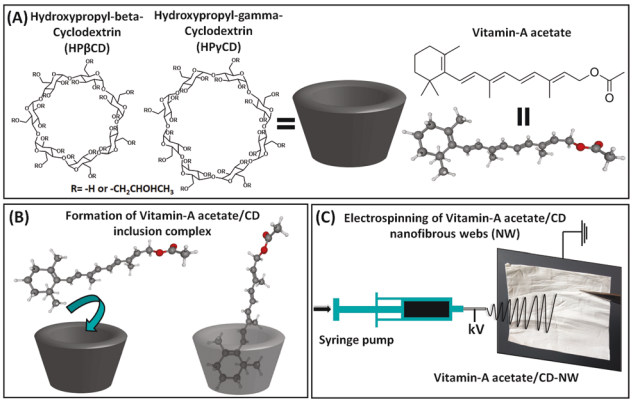


Fig. 1 (A) The chemical structures of HPβCD, HPγCD and Vitamin-A acetate. Schematic illustrations of (B) Vitamin-A acetate and CD inclusion complex formation and (C) the electrospinning of Vitamin-A acetate/CD-NW.

## 2. Materials and methods

### 2.1. Materials

HPβCD (Cavasol W7 HP, DS ~ 0.9) and HPγCD (Cavasol W8 HP Pharma, DS ~ 0.6) were presented by Wacker Chemie AG (USA). Vitamin-A acetate (retinol acetate, Sigma Aldrich), methanol (≥99.8% (GC), Sigma Aldrich), 2,2-diphenyl-1-picrylhydrazyl (DPPH, ≥97%, TCI America), sodium chloride (NaCl, >99%, Sigma Aldrich), *o*-phosphoric acid (85% (HPLC)), potassium phosphate monobasic ($KH_2PO_4$, ≥99.0%, Fisher Chemical), sodium phosphate dibasic heptahydrate ($Na_2HPO_4$, 98.0–102.0%, Fisher Chemical), and deuterated dimethylsulfoxide ($d_6$-DMSO, 99.8%, Cambridge Isotope) were purchased and used as received. A Millipore Milli-Q ultrapure water system (Millipore, USA) was used to supply high-quality distilled water.

### 2.2. Electrospinning

For both pristine CD nanofibers and Vitamin-A acetate/CD nanofibrous webs (NW), clear HPβCD and HPγCD solutions were initially prepared in distilled water at a 200% (w/v) CD concentration. In the case of Vitamin-A acetate/CD-NW, Vitamin-A acetate powder was added to HPβCD and HPγCD solutions separately. The molar ratio of the Vitamin-A acetate/CD solutions was arranged as 1 : 2 (Vitamin-A acetate : CD) which corresponds to ~10% (w/w, with respect to total sample amount) (~1 g CD and ~0.1 g Vitamin-A acetate) of Vitamin-A acetate content in Vitamin-A acetate/CD-NW. To ensure inclusion complex formation, Vitamin-A acetate/CD aqueous systems were stirred for 24 hours (RT) by shielding from light sources. Prior to electrospinning, the conductivity (conductivity meter; FiveEasy, Mettler Toledo, USA) and the viscosity (rheometer; AR 2000 rheometer, TA Instruments, USA (20 mm cone/plate spindle (CP 20–4, 4°); 0.01–1000 $s^{-1}$; 21 °C)) of CD and Vitamin-A acetate/CD solutions were measured precisely. Electrospinning process was performed using electrospinning equipment (Spingenix, model SG100, Palo Alto, USA). The

solutions were filled into plastic syringes, each fitted with a 21 G metallic needle. Process parameters of flow rate, tip-to-collector distance, and high voltage were 0.5 mL $h^{-1}$, 12 cm and 15 kV, respectively (20 °C, 50% relative humidity). Physical mixtures of Vitamin-A acetate/CD were prepared for comparison, as well. Here, pristine HPβCD-NW and HPγCD-NW (~25 mg) were homogenously blended with Vitamin-A acetate powder (~2.7 mg) to obtain Vitamin-A acetate/CD physical mixtures (PM) with the same molar ratio of 1 : 2 (Vitamin-A acetate : CD) used for the preparation of the electrospinning system. The samples were stored at ambient conditions (20 °C, 50% relative humidity) during the analyses.

### 2.3. Morphology analyses

The morphologies of electrospun HPβCD-NW, HPγCD-NW, Vitamin-A acetate/HPβCD-NW and Vitamin-A acetate/HPγCD-NW were analyzed using a scanning electron microscope (SEM, Tescan MIRA3, Czech Republic) in high vacuum. A small piece of each sample was fixed onto SEM stubs by double-sided carbon tape and sputter-coated with Au/Pd. For SEM imaging, the working distance was set to 10 mm and the accelerating voltage was 10 kV. The average diameter (AD) of nanofibers was calculated by the measurement of numerous fibers (~100) using ImageJ software.

### 2.4. Structural characterization

An attenuated total reflectance Fourier transform infrared (ATR-FTIR) spectrometer (PerkinElmer, USA) was used to obtain FTIR spectra of samples. The FTIR spectra were recorded in the 4000–600 $cm^{-1}$ region (resolution of 4 $cm^{-1}$) with 64 scans. An X-ray diffractometer (Bruker D8 Advance ECO, USA) was used to investigate the X-ray diffraction patterns of the samples. A Cu-Kα radiation source was used to form the XRD graphs ($2\theta$ angles: 5° and 30°) and voltage/current values were set to 40 kV/25 mA. The thermograms of samples were obtained using a differential scanning calorimeter (DSC, Q2000, TA Instruments, USA) (0–240 °C; 10 °C $min^{-1}$; $N_2$). A thermogravimetric analyzer (TGA, Q500, TA Instruments, USA) was utilized to determine the thermogravimetric profiles of samples (RT to 600 °C; 20 °C $min^{-1}$; $N_2$). A nuclear magnetic resonance spectrometer (Bruker AV500, with autosampler, USA) was utilized to calculate the molar ratio between Vitamin-A acetate and CD in Vitamin-A acetate/CD-NW. $d_6$-DMSO was used as the solvent to dissolve samples for proton nuclear magnetic resonance ($^1$H-NMR) measurements. The samples (~40 mg) were dissolved in $d_6$-DMSO (~500 μL) and then they were loaded into instruments and $^1$H-NMR spectra were recorded with 16 scans. The chemical shifts ($\delta$, ppm) of each sample were processed using Mestranova software.

### 2.5. Dissolution/disintegration, release, and phase solubility studies

For the examination of dissolution profiles, ~10 mg of nanofibrous webs of pristine CD and Vitamin-A acetate/CD, and ~1 mg Vitamin-A acetate powder were loaded into glass vials, separately. Then, 5 mL of distilled water was poured into these vials in sequence (Video S1†). Here, the solubility enhancement of Vitamin-A acetate encapsulated in Vitamin-A acetate/CD-NW was also demonstrated spectroscopically (see ESI†). The time-dependent release test of Vitamin-A acetate in Vitamin-A acetate/CD-NW (20 mg) was performed in distilled water (20 mL) at room temperature. For control, Vitamin-A acetate (~2 mg) powder was also examined using the initial Vitamin-A acetate content in nanofibrous webs. Here, Vitamin-A acetate/CD-NW and Vitamin-A acetate powder were placed into a beaker, after which liquid medium was poured in. While the solution systems were being shaken (200 rpm), 500 μL of sample solution was withdrawn and then fresh medium (500 μL) was refilled at the determined time points. The released amount of Vitamin-A acetate was analyzed using UV-visible spectroscopy (PerkinElmer, Lambda 35, USA). The calibration curve of Vitamin-A acetate showed linearity and acceptability with $R^2 \geq 0.99$. The measurement results were converted into released % by using this calibration curve. The experiments were performed three times and results were reported as mean ± standard deviation. To evaluate the kinetic profile of samples, various mathematical models were applied, including zero- and first-order release model, Higuchi release model and Korsmeyer–Peppas equation (see ESI†).[48]

The disintegration profiles of Vitamin-A acetate/HPβCD-NW and Vitamin-A acetate/HPγCD-NW were followed using a modified version of a technique which was previously reported by Bi *et al.*[49] In this approach, the physiological circumstances of the surface of a moist tongue are simulated. In this study, filter paper was firstly located in a plastic Petri dish (10 cm), and then wetted with artificial saliva (10 mL). 1.19 g $Na_2HPO_4$, 0.095 g $KH_2PO_4$ and 4 g NaCl were mixed in 500 mL distilled water and its pH was arranged to 6.8 with phosphoric acid to prepare artificial saliva. The extra artificial saliva was withdrawn from the Petri dish and Vitamin-A acetate/CD-NW with approximate dimensions of 3 cm × 5 cm was put at the centre of the filter paper (Video S2†).

The phase solubility profiles of Vitamin-A acetate/HPβCD and Vitamin-A acetate/HPγCD systems were determined by a technique reported previously.[50] An excess amount of Vitamin-A acetate and CD (HPβCD and HPγCD) powder with an increasing concentration from 0 to 40 mM were weighted into glass vials, separately. Afterwards, water (5 mL) was added to each of the vials, and they were sealed and shaken for 24 hours on an incubator shaker (25 °C and 450 rpm) by shielding from the light. A PTFE filter (0.45 μm) was used to filter the incubated suspensions. UV-visible spectroscopy was used to measure the absorbance of the filtered aliquots. The experiments were conducted three times ($n$ = 3) and the phase solubility diagrams were plotted using the average absorption results. The binding constants ($K_s$) were determined from the following equation:

$$K_s = \text{slope}/S_0(1 - \text{slope}) \quad (1)$$

where $S_0$ is the intrinsic solubility of Vitamin-A acetate (~7.25 μM) in the absence of CD.

 

### 2.6. Antioxidant activity test

The antioxidant activities of Vitamin-A acetate powder, Vitamin-A acetate/CD-NW and Vitamin-A acetate/CD-PM were examined using the DPPH radical scavenging technique. For antioxidant experiments, Vitamin-A acetate/CD-NW (~30 mg), Vitamin-A acetate/CD-PM (~30 mg) and Vitamin-A acetate powder (~3 mg) were stirred in 2 mL of distilled water for 1 hour at 150 rpm. Then, all aqueous systems were filtered by a PTFE filter (0.45 μm) to remove the undissolved Vitamin-A acetate parts in the solutions. Afterwards, 1 mL of the filtered solution of sample and 2 mL of 75 μM concentrated methanolic DPPH solution were mixed and incubated in the dark. UV-visible measurements were carried out at different incubation time intervals and the disappearance of DPPH absorption (517 nm) was followed to evaluate the inhibition performance of samples. Each experiment was performed three times and the radical scavenging performance of samples was represented as inhibition percentage by using the following equation:

$$\text{Inhibition } (\%) = (A_{\text{control}} - A_{\text{sample}})/A_{\text{control}} \times 100 \qquad (2)$$

where $A_{\text{control}}$ stands for the absorbance value of control DPPH solution and $A_{\text{sample}}$ stands for that of the sample solution.

### 2.7. Statistical analyses

The results of the replicated experiment ($n \geq 3$) were stated as mean values ± standard deviations. The statistical analyses were performed using one-way or two-way analysis of variance (ANOVA). ANOVA was carried out by OriginLab (Origin 2020, USA) (0.05 level of probability).

## 3. Results and discussion

### 3.1. Morphology analysis

Vitamin-A acetate molecules present a lipophilic characteristic due to the cyclohexene ring and polyenic chain in the structure (Fig. 1).[41] The lipophilic nature of Vitamin-A acetate is the major driving force for inclusion complex formation with CD molecules and, as was reported previously, the hydrophobic cyclohexene ring of Vitamin-A acetate is preferably encapsulated into the apolar cavity of CD in the event of inclusion complexation.[41] In the case of hydroxypropyl derivatives of CD, the extended cavity of CD enables the encapsulation of cyclohexene ring into the CD cavity; however, the repulsion forces between the hydroxypropyl groups of CD and bended polyenic chain of Vitamin-A acetate can inhibit the effective association.[41] As such, for the interaction between Vitamin-A acetate and hydroxypropylated derivatives of CD, a 1 : 2 molar ratio (Vitamin-A acetate : CD) has been recorded as more favorable in which higher amount of CD molecules is used for the complex formation compared to 1 : 1 molar ratio (Vitamin-A acetate : CD).[41] Therefore, we have preferred to prepare Vitamin-A acetate/CD aqueous solutions having 1 : 2 (Vitamin-A acetate : CD) molar ratio for electrospinning. Here, the inclusion complex systems of Vitamin-A acetate/CD were obtained using two different modified CD types of HPβCD and HPγCD. The highly concentrated solutions of CD (200%, w/v) ensure the electrospinning of uniform CD nanofibers; therefore Vitamin-A acetate/CD solutions were also prepared by using 200% (w/v) concentration of HPβCD and HPγCD solutions. As seen in Fig. 2, the clear solutions of HPβCD and HPγCD became a yellowish color by the addition of Vitamin-A acetate. Here, the high concentration and so the very high viscosity of Vitamin-A acetate/CD solutions (200%, w/v) might hinder the efficient mixing of systems in order to attain an efficient inclusion complexation, and so some uncomplexed Vitamin-A acetate might be present in Vitamin-A acetate/CD-NW. Nevertheless, the electrospinning of Vitamin-A acetate/CD aqueous solutions prepared with 1 : 2 molar ratio

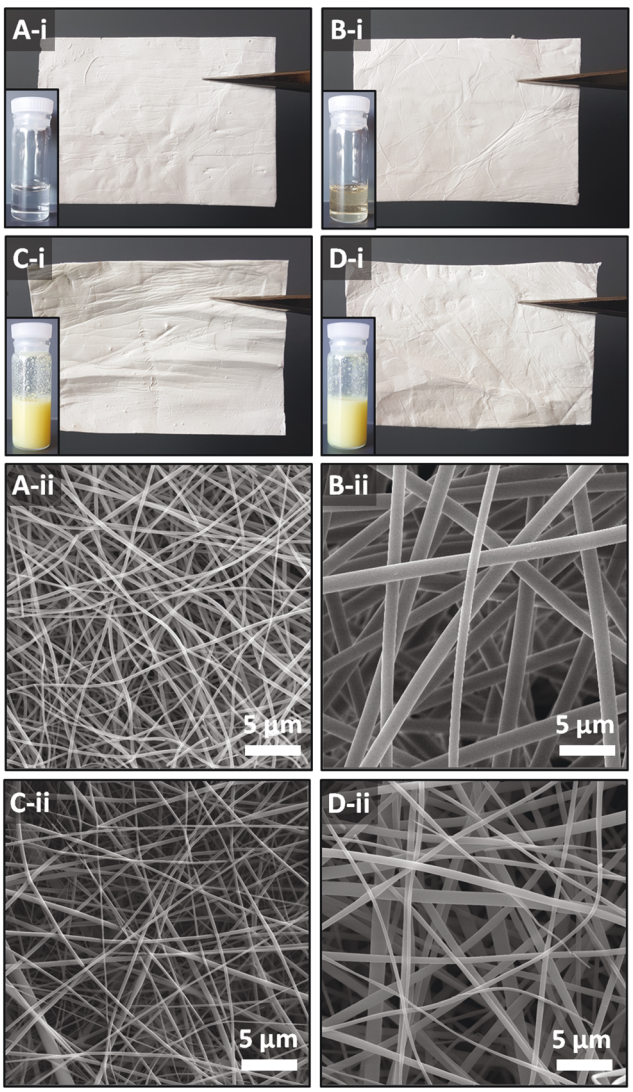


Fig. 2 (i) Photos of the electrospinning solutions and the free-standing webs and (ii) representative SEM images of (A) HPβCD-NW, (B) HPγCD-NW, (C) Vitamin-A acetate/HPβCD-NW and (D) Vitamin-A acetate/HPγCD-NW.

was effective in which uniform electrospun nanofibers of Vitamin-A acetate/HPβCD and Vitamin-A acetate/HPγCD were obtained upon self-standing and with flexible properties (Fig. 2C and D-i). Uniform pristine HPβCD-NW and HPγCD-NW were also produced in the form of self-standing character (Fig. 2A and B-i).

The SEM images depicted that the pristine CD-NW and the Vitamin-A acetate/CD-NW have uniform fibrous structure raised with bead-free morphology (Fig. 2). The solution properties (viscosity and conductivity) of the pristine CD and the Vitamin-A acetate/CD solutions, and the average diameter (AD) of the ultimate nanofibrous webs are given in Table S1.† In electrospinning, solutions having higher viscosity and lower conductivity generally lead to thicker fibers, because the electrospinning jet can be exposed to less stretching compared to solutions having lower viscosity and higher conductivity during the electrospinning process.[51] Pristine HPβCD-NW and Vitamin-A acetate/HPβCD-NW were obtained having AD of 220 ± 60 nm and 195 ± 85 nm, respectively, whereas the electrospinning of pristine HPγCD-NW and Vitamin-A acetate/HPγCD-NW resulted in much thicker fibers having AD of 1260 ± 245 nm and 610 ± 275 nm, respectively. HPβCD-based solutions have higher conductivity along with lower viscosity compared to the HPγCD-based ones which probably provided greater stretching of the electrospinning jet and so led to thinner fiber formation during the process (Table S1†). When pristine CD systems were compared with the Vitamin-A acetate/CD ones, it was observed that there was a decrease in the AD of CD-NW with the addition of Vitamin-A acetate. This might be due to the higher conductivity of Vitamin-A acetate/CD systems which can ensure higher stretching of the jet during the process. In the case of HPβCD systems, the conductivity of Vitamin-A acetate/HPβCD solution was slightly higher than that of pure HPβCD system, and therefore there was no distinct difference between the AD value of HPβCD-NW (220 ± 60 nm) and Vitamin-A acetate/HPβCD-NW (195 ± 85 nm). On the other hand, the variation between the AD of Vitamin-A acetate/HPγCD-NW (1260 ± 245 nm) and HPγCD-NW (610 ± 275 nm) was higher compared to HPβCD-based systems due to the more significant difference between the conductivity values of Vitamin-A acetate/HPγCD and HPγCD solutions (Table S1†). The statistical analyses supported our results in which significant variations were detected between samples ($p < 0.05$).

### 3.2. Structural characterization

FTIR is a commonly used technique to evaluate both inclusion complex formation and the existence of guest molecules in inclusion complex structures.[25,26] The interactions between guest molecules and CD cavities generally lead to disappearance, attenuation and/or shifts in the typical peaks of guest molecules.[52,53] Fig. 3 shows the FTIR spectra of Vitamin-A acetate powder, pristine CD-NW (HPβCD and HPγCD), Vitamin-A acetate/CD-NW (Vitamin-A acetate/HPβCD and Vitamin-A acetate/HPγCD) and Vitamin-A acetate/CD physical mixtures (PM). There are major peaks at around

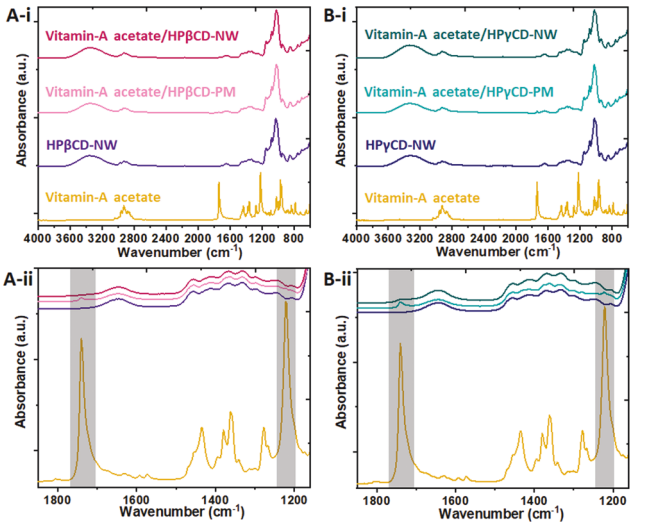


Fig. 3 (i) The full and (ii) the expanded range FTIR spectra of (A) Vitamin-A acetate powder, HPβCD-NW, Vitamin-A acetate/HPβCD-PM and Vitamin-A acetate/HPβCD-NW; (B) Vitamin-A acetate powder, HPγCD-NW, Vitamin-A acetate/HPγCD-PM and Vitamin-A acetate/HPγCD-NW.

3000–3600 $cm^{-1}$ for the primary/secondary –OH stretching, 2930 $cm^{-1}$ for C–H stretching, 1650 $cm^{-1}$ for O–H bending and 1370 $cm^{-1}$ for $-CH_3$ bending vibrations of CDs (Fig. 3A and B-i). The other major absorption bands which are seen between 1020 and 1200 $cm^{-1}$ are owing to coupled C–C/C–O and antisymmetric C–O–C stretching of CD.[54] In the case of Vitamin-A acetate/CD-NW, the characteristic peaks of Vitamin-A acetate are not detectable since they were hindered due the encapsulation into CD cavities by inclusion complexation. On the other hand, the two characteristic peaks of Vitamin-A acetate located at 1220 $cm^{-1}$ and 1740 $cm^{-1}$ corresponding to the stretching of C–C/C–C–H and C═O, respectively, are obvious in the FTIR spectra of Vitamin-A acetate/CD-PM (Fig. 3A and B-ii).[55,56] This observation proved the inclusion complex formation between Vitamin-A acetate and CD molecules in Vitamin-A acetate/CD-NW.

As depicted in Fig. 4A and B, Vitamin-A acetate powder exhibits a crystalline pattern and XRD provides useful information as to whether the Vitamin-A acetate molecules are distributed in the Vitamin-A acetate/CD-NW as crystals or in amorphous state. In other words, the XRD technique gives information about the complex formation between CD and guest molecules, because the guest molecules cannot aggregate to form crystals and separate from each other when they are encapsulated in CD cavities by inclusion complexation.[52] The XRD profiles of Vitamin-A acetate powder, Vitamin-A acetate/CD-NW and Vitamin-A acetate/CD-PM are displayed in Fig. 4A and B. The as-received Vitamin-A acetate powder shows characteristic crystalline diffraction peaks at 9.1°, 17.3°, 18.5°, 20.1° and 24.4°. On the other hand, pristine HPβCD-NW and HPγCD-NW have broad halo XRD patterns due to their amorphous nature (Fig. 4A and B). In the case of Vitamin-A acetate/

 

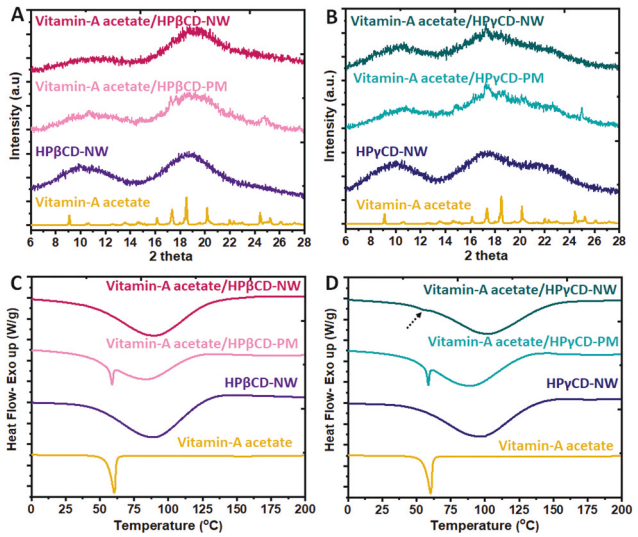


**Fig. 4** (A, B) XRD patterns and (C, D) DSC thermograms of Vitamin-A acetate powder, HPβCD-NW, Vitamin-A acetate/HPβCD-PM, Vitamin-A acetate/HPβCD-NW, HPγCD-NW, Vitamin-A acetate/HPγCD-PM, and Vitamin-A acetate/HPγCD-NW.

CD-PM, the crystalline peaks of Vitamin-A acetate become apparent because of the uncomplexed structure of samples. Despite this, Vitamin-A acetate/HPβCD-NW has an amorphous pattern like pristine HPβCD-NW and Vitamin-A acetate/HPγCD-NW indicates an almost amorphous pattern with weak characteristic peaks (17.3°, 18.5° and 20.1°) of Vitamin-A acetate. The XRD pattern of Vitamin-A acetate/HPγCD-NW showing the characteristic diffraction peaks of Vitamin-A acetate proves the existence of some crystalline form of Vitamin-A acetate in this sample. On the other hand, Vitamin-A acetate was completely in the inclusion complex state in Vitamin-A acetate/HPβCD-NW. The Vitamin-A acetate crystals were not obvious in the SEM images of Vitamin-A acetate/HPγCD-NW (Fig. 2D-ii) implying that the Vitamin-A acetate crystals were most probably distributed in small sizes within the nanofibrous matrix.

The DSC data also demonstrated that Vitamin-A acetate powder is in a crystalline form having a melting peak at 60 °C (Fig. 4C and D). Therefore, DSC analysis was further performed to detect if there was any presence of uncomplexed crystalline Vitamin-A acetate in Vitamin-A acetate/CD-NW. Pristine HPβCD-NW and HPγCD-NW have a broad peak between 30 and 140 °C originated from water loss and since they are amorphous, there is no melting peak observed in the DSC thermograms of these samples.[57] For Vitamin-A acetate/HPβCD-NW, the melting peak of Vitamin-A acetate was not detected confirming the fully inclusion complexed state of Vitamin-A acetate with HPβCD in this sample. The guest molecules are separated from each other and not able to form crystals in the case of inclusion complexation; therefore the characteristic melting peak of guest molecules is not detected in DSC data.[52] On the other hand, the DSC curve of Vitamin-A acetate/HPβCD-PM indicates an endothermic peak at 59 °C with a peak area of 5.8 J $g^{-1}$ (Fig. 4C). In the case of Vitamin-A acetate/HPγCD-NW, there is a very small endothermic peak at 56 °C for melting of Vitamin-A acetate crystals with a peak area of ~0.9 J $g^{-1}$. The physical mixture of Vitamin-A acetate/HPγCD has an endothermic peak at 59 °C with a peak area of 5.1 J $g^{-1}$ (Fig. 4D). This finding revealed that most of the Vitamin-A acetate was inclusion complexed with HPγCD, but there were still uncomplexed Vitamin-A acetate crystals present in Vitamin-A acetate/HPγCD-NW. The DSC results further proved that Vitamin-A acetate was completely in inclusion complex state in Vitamin-A acetate/HPβCD-NW whereas there was uncomplexed crystalline Vitamin-A acetate present in Vitamin-A acetate/HPγCD-NW. Briefly, DSC findings are in good agreement with the XRD data.

The TGA measurements of Vitamin-A acetate powder, pristine CD-NW, Vitamin-A acetate/CD-NW and Vitamin-A acetate/CD-PM were performed by a thermogravimetric analyzer (Fig. 5). Vitamin-A acetate powder displays mass loss that starts at 100 °C and ends up at 500 °C in two degradation steps. Pristine CD-NW has initial weight loss below 100 °C due to the evaporation of water. Pristine HPβCD-NW and HPγCD-NW exhibit main thermal degradation in the ranges of 280–430 °C and 265–420 °C, respectively. The main degradation of Vitamin-A acetate overlaps with the main degradation step of pristine CD (Fig. 5); therefore two steps of mass losses were also observed in the case of Vitamin-A acetate/CD-NW samples. In addition, the first degradation step of Vitamin-A acetate powder, which occurs at lower temperature range (100 °C–276 °C), is not obvious for Vitamin-A acetate/CD-NW and this might be evidence for the inclusion complex formation between Vitamin-A acetate and CD molecules (Fig. 5). The inclusion complexation can principally increase the thermal stability of guest molecules and this is observed by shifting of the thermal degradation step of the guest to

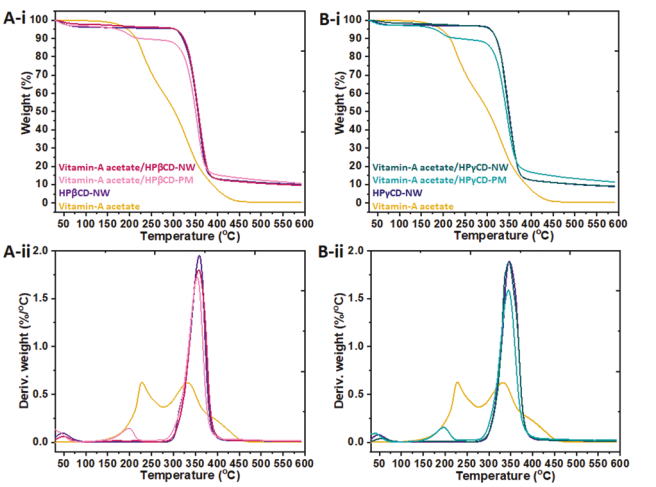


**Fig. 5** TGA thermograms (i) and derivatives (ii) of (A) Vitamin-A acetate, HPβCD-NW, Vitamin-A acetate/HPβCD-NW, Vitamin-A acetate/HPβCD-PM and (B) Vitamin-A acetate, HPγCD-NW, Vitamin-A acetate/HPγCD-NW, Vitamin-A acetate/HPγCD-PM.

higher temperature ranges.[52] On the other hand, the considered degradation step of Vitamin-A acetate is detected for Vitamin-A acetate/CD-PM. In brief, TGA findings validated the interaction between Vitamin-A acetate and CD in Vitamin-A acetate/CD-NW.

In this study, $^1$H-NMR measurements were performed in order to determine the molar ratio between Vitamin-A acetate and CD in Vitamin-A acetate/CD-NW which can be used to calculate the loading efficiency of Vitamin-A acetate/CD-NW (Fig. 6 and Fig. S1†). The electrospinning solution systems of Vitamin-A acetate/CD were prepared with an initial molar ratio of 1 : 2 (Vitamin-A acetate : CD) for both Vitamin-A acetate/HPβCD and Vitamin-A acetate/HPγCD. Here, Vitamin-A acetate powder, Vitamin-A acetate/HPβCD-NW and Vitamin-A acetate/HPγCD-NW were dissolved in $d_6$-DMSO before the $^1$H-NMR measurements. The spectra of the samples are depicted in Fig. 6 and Fig. S1.† The molar ratio between Vitamin-A acetate and CD was calculated by using the integration proportion of the characteristic peaks of Vitamin-A acetate and CD in Vitamin-A acetate/CD-NW. The $-CH_3$ peaks of both Vitamin-A acetate peaks at 1.3–2.1 ppm and modified CDs at 1.03 ppm were used for the calculation of molar ratio. As is seen, the $-CH_3$ peaks of Vitamin-A acetate located at ~1 ppm overlap with the CD ones. Therefore, for this region, the integration value of Vitamin-A acetate was subtracted from the integration value of Vitamin-A acetate/CD-NW during the calculations. The molar ratios of Vitamin-A acetate/HPβCD-NW and Vitamin-A acetate/HPγCD-NW were determined as ~1 : 4 from the $^1$H-NMR peak integrations. The $^1$H-NMR findings indicated that ~50% of the initial Vitamin-A acetate concentration was conserved during the electrospinning of Vitamin-A acetate/CD-NW, and so the ultimate nanofibrous webs were obtained with ~5% (w/w) loading capacity. Here, the highly viscous Vitamin-A acetate/CD solution which was prepared using high CD concentration (200%, w/w) might raise some difficulties during the stirring of the system. Therefore, the initial content of Vitamin-A acetate (~10%, w/w) could not be completely preserved during the preparation steps and some parts of Vitamin-A acetate could not be included into the electrospinning process. On the other hand, the amount of Vitamin-A acetate of ~5% (w/w) loaded into the nanofibrous webs is quite enough to obtain an efficient antioxidant performance as will discussed in the following part. As was addressed in the previous section, there is some uncomplexed Vitamin-A acetate in Vitamin-A acetate/HPγCD-NW; however $d_6$-DMSO enabled the dissolution of both complexed and uncomplexed Vitamin-A acetate present in the nanofibrous webs. It is also worth mentioning that Vitamin-A acetate/HPβCD-NW and Vitamin-A acetate/HPγCD-NW have the same Vitamin-A acetate peaks as pure Vitamin-A acetate powder, which explained that the structure of Vitamin-A acetate was protected during the electrospinning process.

### 3.3. Dissolution, release, and disintegration profile

The fast dissolution profiles of Vitamin-A acetate powder (~1 mg), pristine CD-NW (~10 mg) and Vitamin-A acetate/CD-NW (~10 mg) were visually examined by adding 5 mL of water to the vials which were loaded with the mentioned samples (Fig. 7 and Video S1†). Here, pristine HPβCD-NW and HPγCD-NW disappeared upon contact with water. On the other hand, Vitamin-A acetate did not dissolve and remained on the top of the water over a given period of time because of

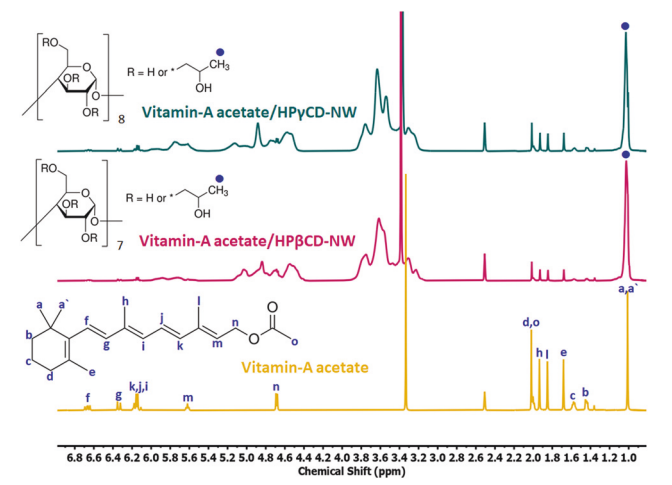


Fig. 6 $^1$H-NMR spectra of Vitamin-A acetate powder, Vitamin-A acetate/HPβCD-NW and Vitamin-A acetate/HPγCD-NW which were recorded by dissolving samples in $d_6$-DMSO.


Fig. 7 The dissolution behavior of samples in water. (A) Vitamin-A acetate powder, (B) HPβCD-NW, (C) Vitamin-A acetate/HPβCD-NW, (D) HPγCD-NW and (E) Vitamin-A acetate/HPγCD-NW. These images were captured from Video S1.†

its almost insoluble nature (Fig. 7). In the case of Vitamin-A acetate/HPβCD-NW, the sample disappeared immediately on the addition of water; however a slightly turbid aqueous system was obtained, since the ultimate complex structure of Vitamin-A acetate/HPβCD most probably had low solubility in water for the tested sample concentration (2 mg $mL^{-1}$). Even so, the Vitamin-A acetate/HPβCD inclusion complexes homogenously dispersed in water (Fig. 7). On the contrary, the uncomplexed and undissolved Vitamin-A acetate content in Vitamin-A acetate/HPγCD-NW was somewhat heterogeneously detected in water. Here, the solubility enhancement of Vitamin-A acetate in Vitamin-A acetate/CD-NW was also indicated using spectroscopic measurement. The same amounts of Vitamin-A acetate powder (~1 mg) and Vitamin-A acetate/CD-NW (~10 mg) were stirred in 5 mL water for 1 hour and then the undissolved parts of Vitamin-A acetate were removed by filtration. Fig. S2† shows the UV-visible absorption spectra of the filtered solutions. It is obvious that Vitamin-A acetate has a very low absorption intensity in the given range because of its quite poor water solubility (~7.5 μM). On the other hand, the solution of Vitamin-A acetate/CD-NW indicated a much higher absorption intensity compared to Vitamin-A acetate powder (Fig. S2†), despite the fact that it contains less Vitamin-A acetate (~0.5 mg) compared to the Vitamin-A acetate powder (~1 mg) used for this experiment. This finding has proved the enhanced solubility of Vitamin-A acetate in Vitamin-A acetate/CD-NW by inclusion complexation. Even though Vitamin-A acetate/HPβCD-NW and Vitamin-A acetate/HPγCD-NW were obtained with the same loading capacity (5%, w/w) of Vitamin-A acetate, the absorption intensity of Vitamin-A acetate/HPβCD solution is higher than that of Vitamin-A acetate/HPγCD (Fig. S2†). The reason for this is the uncomplexed/undissolved Vitamin-A acetate present in Vitamin-A acetate/HPγCD-NW and this suggests that HPβCD can provide a better solubility enhancement for Vitamin-A acetate than HPγCD.

In this study, the time-dependent release profiles of Vitamin-A acetate powder, Vitamin-A acetate/HPβCD-NW and Vitamin-A acetate/HPγCD-NW were examined as well (Fig. 8). The significant improvement of release of Vitamin-A acetate in the nanofibrous webs was demonstrated compared to pure Vitamin-A acetate (Fig. 8). Both Vitamin-A acetate/CD-NW samples dissolved instantly with the contact of liquid medium and showed similar release profiles. Vitamin-A acetate/HPβCD-NW and Vitamin-A acetate/HPγCD-NW respectively released 94.3 ± 4.9% and 55.2 ± 1.3% of the encapsulated Vitamin-A acetate in the first 30 seconds and indicated an approximately steady profile up to 10 minutes. This finding was correlated with the dissolution test in which Vitamin-A acetate/HPγCD-NW showed lower absorption intensity compared to Vitamin-A acetate/HPβCD-NW at the end of 1 hour stirring period (Fig. S2†) due to the uncomplexed/undissolved Vitamin-A acetate part in Vitamin-A acetate/HPγCD-NW. On the other hand, Vitamin-A acetate powder was almost not freed into the liquid medium in this given period (10 minutes, ~0.10 ± 0.07%). These results also confirmed that the

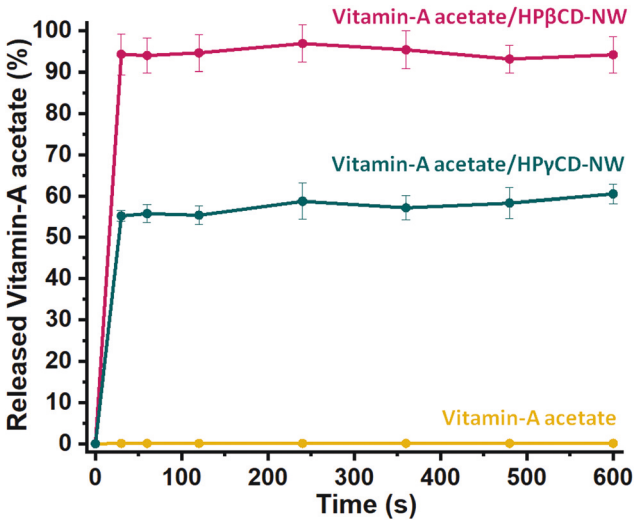


**Fig. 8** Time-dependent release profiles of Vitamin-A acetate powder, Vitamin-A acetate/HPβCD-NW and Vitamin-A acetate/HPγCD-NW.

inclusion complex formation between Vitamin-A acetate and CD within Vitamin-A acetate/CD-NW ensured a distinct enhancement of the release profile of this active compound compared to its pristine form of powder. Here, statistical analyses showed the significant variations between samples with $p < 0.05$. The release behaviors of samples were also evaluated using different kinetic models. The correlation coefficient ($R^2$) values determined by using the equations of kinetic models are summarized in Table S2.† The $R^2$ values revealed that the release behavior of samples fitted with neither zero-/first-order kinetics nor the Higuchi model. These results supported that the release of Vitamin-A acetate from nanofibrous webs was not time dependent and did not happen from a non-soluble matrix in water.[48] On the other hand, results showed higher consistency with the Korsmeyer–Peppas model, also enabling the calculation of the diffusion exponent ($n$) value (Table S2†). For Vitamin-A acetate/CD-NW, the $n$ values were determined in the range of $0.45 < n < 0.89$ suggesting irregular or non-Fickian diffusion which could explain the diffusion and erosion-controlled based release of Vitamin-A acetate from nanofibrous webs.[48] In short, the dissolution and release test findings are also correlated with the XRD and DSC data in which the uncomplexed Vitamin-A acetate in Vitamin-A acetate/HPγCD-NW was detected precisely. As will be addressed in the following section on phase solubility, Vitamin-A acetate forms complexes more favorably with HPβCD compared to HPγCD which might also lead to more efficient inclusion complex formation in the highly concentrated solution of Vitamin-A acetate/HPβCD.

The disintegration of Vitamin-A acetate/CD-NW was further examined on wetted filter paper in order to mimic the oral cavity.[49] Fig. 9 and Video S2† indicate the disintegration profile of Vitamin-A acetate/CD-NW. Both Vitamin-A acetate/HPβCD-NW and Vitamin-A acetate/HPγCD-NW tend to disintegrate upon contact with artificial saliva. Even though Vitamin-

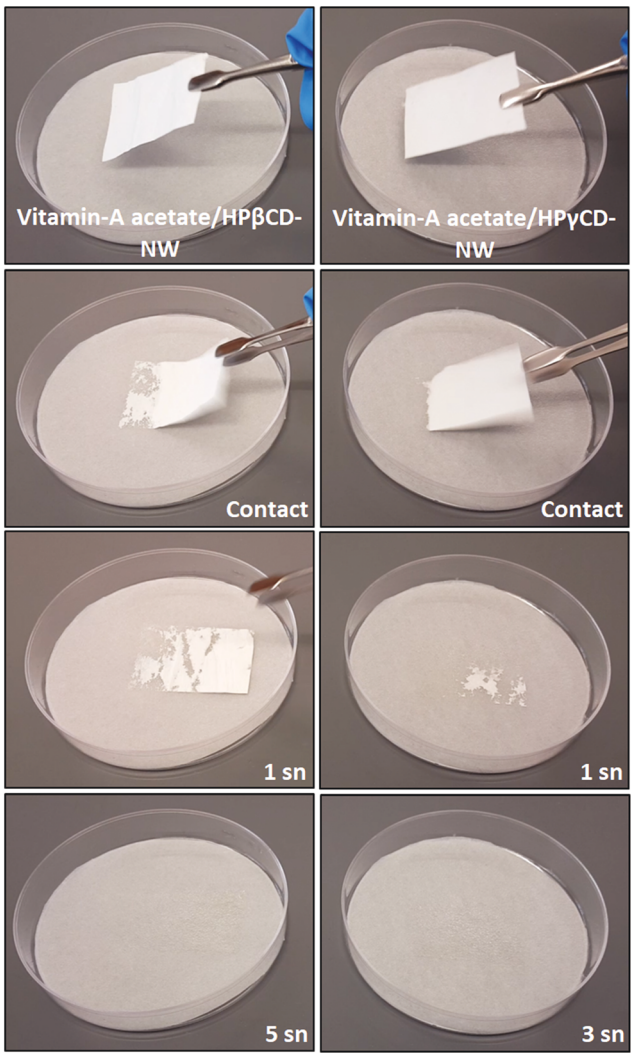


Fig. 9 The disintegration behavior of samples in saliva simulation: Vitamin-A acetate/HPβCD-NW and Vitamin-A acetate/HPγCD-NW. These images were captured from Video S2.†

A acetate/HPγCD-NW contains uncomplexed/crystalline Vitamin-A acetate, this situation was not reflected in the disintegration results. As such, the complete disintegration of Vitamin-A acetate/HPβCD-NW took longer compared to Vitamin-A acetate/HPγCD-NW and the reason might be the less soluble nature of Vitamin-A acetate/HPβCD inclusion complexes compared to Vitamin-A acetate/HPγCD ones, which was also observed in the previous dissolution test. Here, the high water solubility of the hydroxypropylated derivatives of HPβCD and HPγCD is an essential dynamic for the high dissolution and disintegration rate of Vitamin-A acetate/CD-NW.[58] Besides, high surface area and highly porous feature of nanofibrous webs are other key points which ensure the penetration and interaction of water through the nanofibers.[59] Therefore, the nanoporous structure of Vitamin-A acetate/CD-NW can create an easy penetration path for saliva in the mouth, and the highly soluble nature of modified CD (HPβCD and HPγCD) and the inclusion complex entity can facilitate the fast release of Vitamin-A acetate by rapid dissolution of nanofibrous webs.

### 3.4. Phase solubility test

Phase solubility is a precise factor in order to get information about the inclusion stoichiometry, binding constant ($K_s$) and the solubility improvement arising in the case of the interaction between CD and guest molecules.[50,60] Here, the Vitamin-A acetate/CD systems were stirred for 24 hours to provide a proper dynamic equilibrium for inclusion complexation and filtered aliquots of each of these systems were analyzed using a UV-visible spectrometer. Fig. 10A shows the phase solubility diagrams of both Vitamin-A acetate/HPβCD and Vitamin-A acetate/HPγCD systems plotted for the different CD concentrations. It is obvious from the graphs that the solvated Vitamin-A acetate amount increases linearly against increasing CD concentration (0–40 mM). This linear profile represents the AL type phase solubility diagram which reveals inclusion complex formation with 1 : 1 (guest : CD) stoichiometry.[50] On the other hand, as reported previously by Muñoz-Botella *et al.*, Vitamin-A acetate molecules tend to form inclusion complexes with 1 : 2 molar ratio (Vitamin-A acetate : CD) for HPβCD.[41] Depending on this finding, we prepared our electrospinning systems using 1 : 2 molar ratio which was also more feasible for fiber formation from the highly concentrated CD solutions. In the mentioned study, Muñoz-Botella *et al.* examined the stoichiometry of the systems using concentrations of 10 mM for HPβCD and 2–8 mM for Vitamin-A acetate.[41] In our case, the phase solubility analyses were carried out using more diluted Vitamin-A acetate (1 mM) and more concentrated HPβCD (0–40 mM) systems. Therefore, for the experimental conditions that we have used in the phase solubility test, Vitamin-A acetate molecules might interact with the HPβCD cavity in such a way that 1 : 1 complexation takes place. Here, the solubility of Vitamin-A acetate (~7.5 μM) was increased by ~16.1 and ~2.3 times with HPβCD and HPγCD, respectively. Moreover, the binding constant ($K_s$) was determined as 387.8 $M^{-1}$ for Vitamin-A acetate/HPβCD system and 41.4 $M^{-1}$ for Vitamin-A acetate/HPγCD system. These results also demonstrated that Vitamin-A acetate forms more favorable and stable inclusion complexes with HPβCD compared to HPγCD. This most probably originates from the better size match between HPβCD and Vitamin-A acetate which also ensures a better solubility enhancement for Vitamin-A acetate molecules. These findings are also correlated with the previous analyses in which uncomplexed Vitamin-A acetate was detected in the case of Vitamin-A acetate/HPγCD-NW, while Vitamin-A acetate molecules were completely present in the complexed form for Vitamin-A acetate/HPβCD-NW. It is noteworthy that there is a significant variation between samples according to statistical analyses ($p < 0.05$). To the best of our knowledge, the phase solubility test reported by Higuchi and Connors[50] has not been studied for Vitamin-A acetate/CD yet. On the other hand, there are several studies in the literature in which the phase solubility profile of other retinoid derivatives has been evaluated against

 

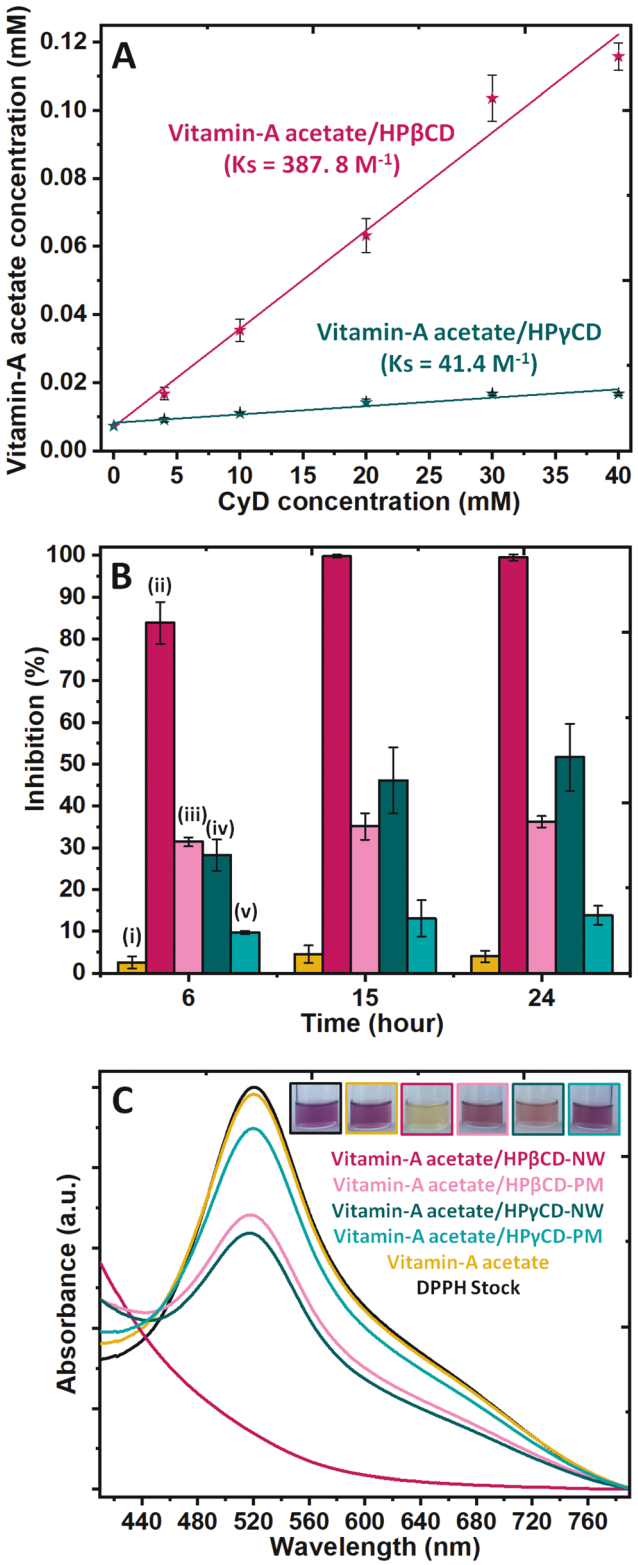


**Fig. 10** (A) Phase solubility diagrams of Vitamin-A acetate/HPβCD and Vitamin-A acetate/HPγCD systems. (B) Time-dependent antioxidant activity graphs of Vitamin-A acetate powder (i), Vitamin-A acetate/HPβCD-NW (ii), Vitamin-A acetate/HPβCD-PM (iii), Vitamin-A acetate/HPγCD-NW (iv) and Vitamin-A acetate/HPγCD-PM (v). (C) Representative UV-visible spectra and photos of aqueous solutions of DPPH stock and samples (24 hours).

HPβCD.[42,43] In these related studies, $K_s$ values were determined as 266.6 $M^{-1}$ and 13 563.2 $M^{-1}$ for all-*trans*-retinoic acid/HPβCD[42] and 13-*cis*-retinoic acid/HPβCD[43] systems, respectively, for a 1 : 1 molar ratio.

### 3.5. Antioxidant activity

Uncontrolled reactive oxygen species and free radicals can create oxidative stresses which induce damage to biochemical compounds including DNA, lipids, and proteins, which may result in cardiovascular diseases, diabetes, cancer, and faster ageing. Antioxidants can scavenge the radical species which are produced continuously in biological systems, and so their destructive effects can be neutralized.[36,39,61] The antioxidant potential of Vitamin-A originates from its hydrophobic polyene chain which has conjugated double bonds and can reduce and stabilize singlet oxygen, free and peroxyl radicals.[39,62] In this study, the antioxidant potentials of Vitamin-A acetate/HPβCD-NW and Vitamin-A acetate/HPγCD-NW were evaluated using DPPH scavenging assay. For control, the antioxidant test was also performed using physical mixtures of Vitamin-A acetate/HPβCD and Vitamin-A acetate/HPγCD and the powder form of Vitamin-A acetate. As reported in our previous study, pristine HPβCD and HPγCD do not have a radical scavenging property.[21] Fig. 10B shows the inhibition graphs of all samples for the different time periods of 6, 15 and 24 hours. Moreover, representative UV-visible absorption spectra of the antioxidant test recorded for 24 hours are depicted in Fig. 10C along with their representative solution photos.

As seen, the antioxidant activity of each sample increases slightly in 15 hours and the scavenging performance of Vitamin-A acetate/HPβCD-NW has stabilized by reaching an inhibition value of ~100%. It is also obvious that there is no distinct difference between 15- and 24-hours results for other samples, as well. These findings are also represented by UV-visible spectra in which the absorption intensity of DPPH at 517 nm decreased or disappeared and the color of the solutions turned to yellow/yellow-purple depending on the scavenging performance of the samples (Fig. 10C). Vitamin-A acetate has quite poor solubility in water, so it exhibited quite low antioxidant activity with maximum 4.5 ± 2.0% inhibition in the given period (Fig. 10B). On the other hand, Vitamin-A acetate/HPβCD-NW and Vitamin-A acetate/HPγCD-NW showed 99.8 ± 0.3% and 51.6 ± 8.0% antioxidant activity, respectively, due to inclusion complexation. Briefly, Vitamin-A acetate/HPβCD-NW provided the maximum antioxidant activity of ~100% and Vitamin-A acetate/HPγCD-NW showed lower performance (51.6 ± 8.0%) for the same sample amount (~30 mg). As was discussed for the previous analyses, there is uncomplexed Vitamin-A acetate in Vitamin-A acetate/HPγCD-NW and this part could not contribute to the radical scavenging, since it was removed by the filtration prior to the incubation period. This finding is also correlated with the phase solubility, dissolution and release test results, where HPβCD-based samples exhibited higher solubilizing effect and release % for Vitamin-A acetate compared to HPγCD-based samples due to more favorable complex formation between

Vitamin-A acetate and HPβCD. As observed in Fig. 10B and C, the physical mixtures of Vitamin-A acetate/HPβCD (36.3 ± 1.3%) and Vitamin-A acetate/HPγCD (13.8 ± 2.3%) exhibited lower antioxidant activity compared to Vitamin-A acetate/CD-NW because of the uncomplexed state of Vitamin-A acetate present in the physical mixtures. Even so, the antioxidant performance of the physical mixtures might be considered higher than it was supposed to be, because the physical mixtures of Vitamin-A acetate/CD have higher antioxidant performance than pure Vitamin-A acetate (4.5 ± 2.0%). However, it should not be forgotten that the physical mixtures have been prepared with an initial Vitamin-A acetate content of ~10% (w/w), while Vitamin-A acetate/CD-NW samples have been obtained with a Vitamin-A acetate content of ~5% (w/w). Thus, even though Vitamin-A acetate/CD-NW contain lower amount of Vitamin-A acetate compared to their physical mixtures, they exhibited higher antioxidant activity. The reason for the better performance of physical mixtures compared to pristine Vitamin-A acetate powder might be also due to the Vitamin-A acetate/CD inclusion complexes formed during the stirring of the physical mixtures which was performed prior to the incubation. The formed Vitamin-A acetate/CD inclusion complexes in the solution of physical mixtures were most probably not removed by the filtration and they took part in the scavenging process. As expected, the higher complexation efficiency of HPβCD has also showed its effect in the case of physical mixtures and Vitamin-A acetate/HPβCD system (36.3 ± 1.3%) exhibited higher performance than Vitamin-A acetate/HPγCD system (13.8 ± 2.3%). To conclude, the complex formation with CD cavities provided an enhanced solubility and stabilization for Vitamin-A acetate and so higher amount of active compound could join the inhibition of DPPH radicals and this suggests the improved antioxidant performance of Vitamin-A acetate. The statistical analyses demonstrated the significant variations between samples ($p < 0.05$).

## 4. Conclusions

To conclude, electrospinning is a feasible method in order to encapsulate different kinds of active compounds in nanofibrous webs. On the other hand, the solubility, stability, and bioavailability of these active compounds can be improved by forming inclusion complexes with CD molecules. The combination of these two phenomena enables one to produce functional nanofibrous webs from the CD inclusion complexes of a variety of compounds which can be utilized as encapsulation systems and can offer enhanced properties for these active compounds by complexation. Here, polymer-free inclusion complex nanofibers of Vitamin-A acetate were obtained using two different derivatives of CD (HPβCD and HPγCD). For both CD types, self-standing nanofibrous webs were obtained with uniform morphology. The loading capacity of the ultimate Vitamin-A acetate/CD-NW was determined as 5% (w/w, with respect to total sample amount). The water solubility of the poorly soluble Vitamin-A acetate has been significantly improved in the case of both HPβCD and HPγCD nanofiber systems. Additionally, both types of Vitamin-A acetate/CD-NW exhibited fast release profiles in liquid medium and fast disintegration profiles in saliva simulation. Moreover, the antioxidant property of Vitamin-A acetate was meaningfully enhanced in the case of Vitamin-A acetate/CD-NW. It was found that HPβCD forms more favorable inclusion complexes with Vitamin-A acetate, and so it provides distinctly greater improvement for both the water solubility and antioxidant property of Vitamin-A acetate compared to HPγCD. Additionally, the polymer-free Vitamin-A acetate/CD-NWs produced in water without using an additional toxic solvent or chemicals are quite promising materials for food- and pharmaceutical-based applications. Here, we have reported the generation of polymer-free electrospun nanofibrous webs of Vitamin-A acetate/CD inclusion complexes which have free-standing, flexible, lightweight, and foldable characteristics. In this study, we aimed to integrate the unique properties of both CD inclusion complexes and electrospun nanofibers to develop a new generation of food/dietary supplements having orally fast-dissolving properties and a nanofibrous web structure.

## Conflicts of interest

There are no conflicts of interest to declare.

## Acknowledgements

This work made use of the Cornell Center for Materials Research Shared Facilities which are supported through the NSF MRSEC program (DMR-1719875), and the Cornell Chemistry NMR Facility supported in part by the NSF MRI program (CHE-1531632), and the Department of Fiber Science & Apparel Design facilities. Prof. Uyar acknowledges the startup funding from the College of Human Ecology at Cornell University. Partial funding for this research was also graciously provided by Nixon Family (Lea and John Nixon) through the College of Human Ecology at Cornell University.

## References

1 M. I. Dias, I. C. F. R. Ferreira and M. F. Barreiro, *Food Funct.*, 2015, **6**, 1035–1052.
2 G. Wadhwa, S. Kumar, L. Chhabra, S. Mahant and R. Rao, *J. Inclusion Phenom. Macrocyclic Chem.*, 2017, **89**, 39–58.
3 P. N. Ezhilarasi, P. Karthik, N. Chhanwal and C. Anandharamakrishnan, *Food Bioprocess Technol.*, 2013, **6**, 628–647.
4 J. A. Bhushani and C. Anandharamakrishnan, *Trends Food Sci. Technol.*, 2014, **38**, 21–33.
5 P. Wen, Y. Wen, M.-H. Zong, R. J. Linhardt and H. Wu, *J. Agric. Food Chem.*, 2017, **65**, 9161–9179.

 

6 M. R. Rostami, M. Yousefi, A. Khezerlou, M. A. Mohammadi and S. M. Jafari, *Food Hydrocolloids*, 2019, **97**, 105170.
7 P. Wen, M.-H. Zong, R. J. Linhardt, K. Feng and H. Wu, *Trends Food Sci. Technol.*, 2017, **70**, 56–68.
8 R. Leidy and Q.-C. M. Ximena, *Trends Food Sci. Technol.*, 2019, **85**, 92–106.
9 T. S. M. Kumar, K. S. Kumar, N. Rajini, S. Siengchin, N. Ayrilmis and A. V. Rajulu, *Composites, Part B*, 2019, 107074.
10 T. D. Brown, P. D. Dalton and D. W. Hutmacher, *Prog. Polym. Sci.*, 2016, **56**, 116–166.
11 J. Xue, T. Wu, Y. Dai and Y. Xia, *Chem. Rev.*, 2019, **119**, 5298–5415.
12 A. Celebioglu, Z. I. Yildiz and T. Uyar, *J. Agric. Food Chem.*, 2018, **66**, 457–466.
13 A. Celebioglu, Z. I. Yildiz and T. Uyar, *Food Res. Int.*, 2018, **106**, 280–290.
14 A. Celebioglu, Z. Aytac, M. E. Kilic, E. Durgun and T. Uyar, *J. Mater. Sci.*, 2018, **53**, 5436–5449.
15 A. Celebioglu, Z. I. Yildiz and T. Uyar, *Int. J. Food Sci. Technol.*, 2018, **53**, 112–120.
16 Z. Aytac, A. Celebioglu, Z. Yildiz and T. Uyar, *Nanomaterials*, 2018, **8**, 793.
17 Z. I. Yildiz, A. Celebioglu, M. E. Kilic, E. Durgun and T. Uyar, *J. Mater. Sci.*, 2018, **53**, 15837–15849.
18 Z. I. Yildiz, A. Celebioglu, M. E. Kilic, E. Durgun and T. Uyar, *J. Food Eng.*, 2018, **224**, 27–36.
19 A. Celebioglu, F. Kayaci-Senirmak, S. İpek, E. Durgun and T. Uyar, *Food Funct.*, 2016, **7**, 3141–3153.
20 A. Celebioglu and T. Uyar, *J. Agric. Food Chem.*, 2017, **65**, 5404–5412.
21 A. Celebioglu and T. Uyar, *Food Chem.*, 2020, **317**, 126397.
22 A. Celebioglu and T. Uyar, *J. Agric. Food Chem.*, 2019, **67**, 13093–13107.
23 A. Celebioglu and T. Uyar, *Int. J. Pharm.*, 2020, 119395.
24 A. Celebioglu and T. Uyar, *RSC Med. Chem.*, 2020, **11**, 245–258.
25 A. Celebioglu and T. Uyar, *Int. J. Pharm.*, 2019, 118828.
26 A. Celebioglu and T. Uyar, *Mol. Pharm.*, 2019, **16**, 4387–4398.
27 Z. I. Yildiz, A. Celebioglu and T. Uyar, *Int. J. Pharm.*, 2017, **531**, 550–558.
28 G. Astray, C. Gonzalez-Barreiro, J. C. Mejuto, R. Rial-Otero and J. Simal-Gandara, *Food Hydrocolloids*, 2009, **23**, 1631–1640.
29 P. Jansook, N. Ogawa and T. Loftsson, *Int. J. Pharm.*, 2018, **535**, 272–284.
30 H. M. C. Marques, *Flavour Fragrance J.*, 2010, **25**, 313–326.
31 E. Fenyvesi, M. Vikmon and L. Szente, *Crit. Rev. Food Sci. Nutr.*, 2016, **56**, 1981–2004.
32 G. F. Combs Jr. and J. P. McClung, *The vitamins: fundamental aspects in nutrition and health*, Academic press, 2016.
33 Y. O. Li, V. P. D. González and L. L. Diosady, in *Microencapsulation in the Food Industry*, Elsevier, 2014, pp. 501–522.
34 A. J. Meléndez-Martínez, *Mol. Nutr. Food Res.*, 2019, **63**, 1801045.
35 I. T. Khan, M. Nadeem, M. Imran, R. Ullah, M. Ajmal and M. H. Jaspal, *Lipids Health Dis.*, 2019, **18**, 41.
36 X. Wu, J. Cheng and X. Wang, *Nutr. Cancer*, 2017, **69**, 521–533.
37 S. Iqbal and I. Naseem, *Nutrition*, 2015, **31**, 901–907.
38 W. Chen, S. Zhao, W. Zhu, L. Wu and X. Chen, *Arch. Immunol. Ther. Exp.*, 2019, 1–11.
39 V. P. Palace, N. Khaper, Q. Qin and P. K. Singal, *Free Radicals Biol. Med.*, 1999, **26**, 746–761.
40 E. Pinho, M. Grootveld, G. Soares and M. Henriques, *Carbohydr. Polym.*, 2014, **101**, 121–135.
41 S. Muñoz-Botella, M. A. Martın, B. Del Castillo, D. A. Lerner and J. C. Menendez, *Anal. Chim. Acta*, 2002, **468**, 161–170.
42 H. Lin, S. Y. Chan, K. S. Y. Low, M. L. Shoon and P. C. Ho, *J. Pharm. Sci.*, 2000, **89**, 260–267.
43 K. L. Yap, X. Liu, J. C. Thenmozhiyal and P. C. Ho, *Eur. J. Pharm. Sci.*, 2005, **25**, 49–56.
44 P. Taepaiboon, U. Rungsardthong and P. Supaphol, *Eur. J. Pharm. Biopharm.*, 2007, **67**, 387–397.
45 H. Li, M. Wang, G. R. Williams, J. Wu, X. Sun, Y. Lv and L.-M. Zhu, *RSC Adv.*, 2016, **6**, 50267–50277.
46 A. Fahami and M. Fathi, *Food Hydrocolloids*, 2018, **81**, 31–38.
47 S. M. Lemma, M. Scampicchio, P. J. Mahon, I. Sbarski, J. Wang and P. Kingshott, *J. Agric. Food Chem.*, 2015, **63**, 3481–3488.
48 N. A. Peppas and B. Narasimhan, *J. Controlled Release*, 2014, **190**, 75–81.
49 Y. Bi, H. Sunada, Y. Yonezawa, K. Danjo, A. Otsuka and K. IIDA, *Chem. Pharm. Bull.*, 1996, **44**, 2121–2127.
50 T. Higuchi and K. A. Connors, *Adv. Anal. Chem. Instrum.*, 1965, **4**, 117–212.
51 T. Uyar and F. Besenbacher, *Polymer*, 2008, **49**, 5336–5343.
52 G. Narayanan, R. Boy, B. S. Gupta and A. E. Tonelli, *Polym. Test.*, 2017, **62**, 402–439.
53 P. Mura, *J. Pharm. Biomed. Anal.*, 2015, **113**, 226–238.
54 C. Yuan, B. Liu and H. Liu, *Carbohydr. Polym.*, 2015, **118**, 36–40.
55 E. I. Taha, S. Al-Saidan, A. M. Samy and M. A. Khan, *Int. J. Pharm.*, 2004, **285**, 109–119.
56 N. L. Rockley, M. G. Rockley, B. A. Halley and E. C. Nelson, in *Methods in enzymology*, Elsevier, 1986, vol. 123, pp. 92–101.
57 A. Celebioglu and T. Uyar, *Nanoscale*, 2012, **4**, 621–631.
58 T. Loftsson and M. E. Brewster, *J. Pharm. Pharmacol.*, 2010, **62**, 1607–1621.
59 D.-G. Yu, J.-J. Li, G. R. Williams and M. Zhao, *J. Controlled Release*, 2018, **292**, 91–110.
60 M. E. Brewster and T. Loftsson, *Adv. Drug Delivery Rev.*, 2007, **59**, 645–666.
61 I. Gülçin, *Arch. Toxicol.*, 2012, **86**, 345–391.
62 C. Grażyna, C. Hanna, A. Adam and B. M. Magdalena, *Int. J. Dairy Technol.*, 2017, **70**, 165–178.